G. BRESSAN (*) & G.F. GENTILE (*)

A STUDY ON FAULTING PATTERN OF EARTHQUAKE AFTERSHOCKS

INDEX

ABSTRACT

The spatial evolution of two aftershock sequences from the Friuli area, clustered both in space and time, are examined.

The aftershock sequences are divided into subsequences arranged in temporal order. For each subsequence, all the combinations of a fixed number of earthquakes are taken, and the scatter matrix of the coordinates of the events, with respect to their centroid, are calculated. The scatter matrices are selected to obtain the best fitting plane where hypocentres are located. The aftershock sequences are mostly characterized by complex multiple faulting. This geometry is probably caused by the stress focusing of the main shock faulting with the subsequent reorientation of the main tectonic axes.

RIASSUNTO

Nel presente lavoro viene esaminata l'evoluzione spaziale di due sequenze sismiche distribuite spazialmente a grappolo e ravvicinate nel tempo.

Le repliche sismiche sono divise in sotto-sequenze, organizzate secondo ordine temporale. Per ciascuna sotto-sequenza si considerano tutte le combinazioni possibili di un numero fissato di terremoti. Per ciascuna combinazione si calcola la matrice di dispersione delle coordinate degli eventi rispetto al centro di massa. Tali matrici di dispersione sono selezionate con opportune procedure per ottenere il migliore piano interpolato dove gli ipocentri degli eventi sono localizzati. Si può notare che le sequenze sismiche di replica sono per lo più caratterizzate da complesso fagliamento multiplo. Tale geometria è probabilmente causata da una concentrazione di sforzo indotta dalla scossa principale e dalla conseguente riorientazione degli assi principali di sforzo tettonico.

KEY WORDS: Aftershocks, active faulting, focal mechanism, stress propagation.

PAROLE CHIAVE: Repliche sismiche, fagliamento attivo, meccanismo focale, propagazione di sforzo.

INTRODUCTION

Most earthquake sequences are clustered both in space and time, suggesting that earthquake foci originate from multiple activated fractures. So a single-plane model appears inadequate to explain the seismicity distribution and to resolve the structure of a seismogenic zone.

The dynamic loading induced by the mainshock causes a concentration of stress in the proximity of the main rupture plane, resulting in complicated aftershock patterns.

SCHOLZ (1988), explained the mechanism of aftershocks as a process of stress relaxation following the mainshock. Since that rock strength increases with strain rate, the dynamic loading induced by the main shock loads the neighbouring rock volume to stresses much higher than their long-term strength. According to this model, rocks fail by static fatigue with a characteristic time delay.

YAMASHITA and KNOPOFF (1987) proposed two models to describe aftershocks occurence (Fig. 1a,b). In model I, irregular slippage is assumed on the fault plane of the main shock, with asperities remaining unbroken after the slippage. The asperities represent the aftershock sources some time after the main shock. In this model, the aftershocks are located in the main rupture plane. In model II, the fracture surface of the main shock is separated from the surrounding auxiliary cracks by barriers where high stress concentrations occur. The

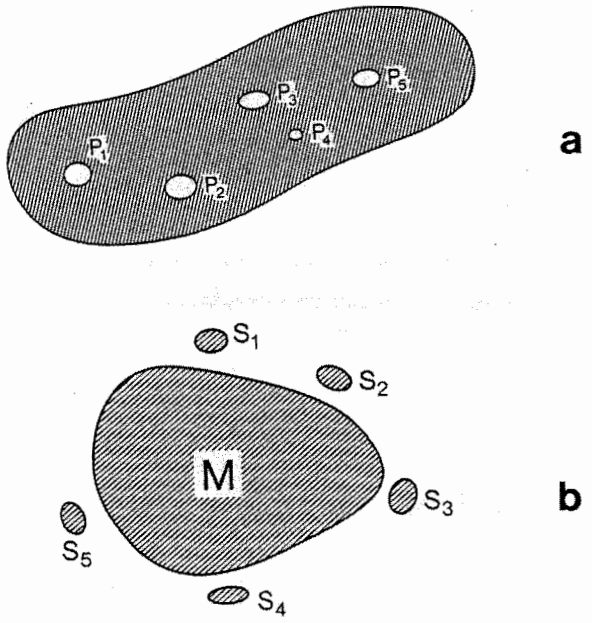

Fig. 1 - Models of aftershock occurrence. a) Model I. Shaded area: fault plane of the main shock. Pi are the asperities where aftershocks occur. b) Model II. Shaded area M: fault plane of the main shock. Si are the auxiliary cracks which surround the fault plane (from YAMASHITA & KNOPOFF,1987).

(*) Osservatorio Geofisico Sperimentale, Trieste (Italy)

interaction of stresses and cracks leads to coalescence of cracks and to aftershock activity. In this model, the aftershocks mainly occur near the edges of the main shock rupture and their locations are strongly influenced by stress focusing caused by the main faulting.

In this paper, an analysis of the spatial distribution of two aftershock sequences in the Friuli area (Fig. 2), using successive events, is performed to

located inside the inner wedge. Its tectonic setting is the product of a complex interference pattern between the Southern Alps and the Dinarides, according to DOGLIONI and BOSELLINI (1987), resulting in low angle, south-verging thrusts, striking E-W (Alpine thrusts), and buried thrusts with SW vergence (Dinaric thrusts). The Dinaric thrusts originated from ENE-WSW compression during the meso-Alpine phase (Eocene). Later, a N-S

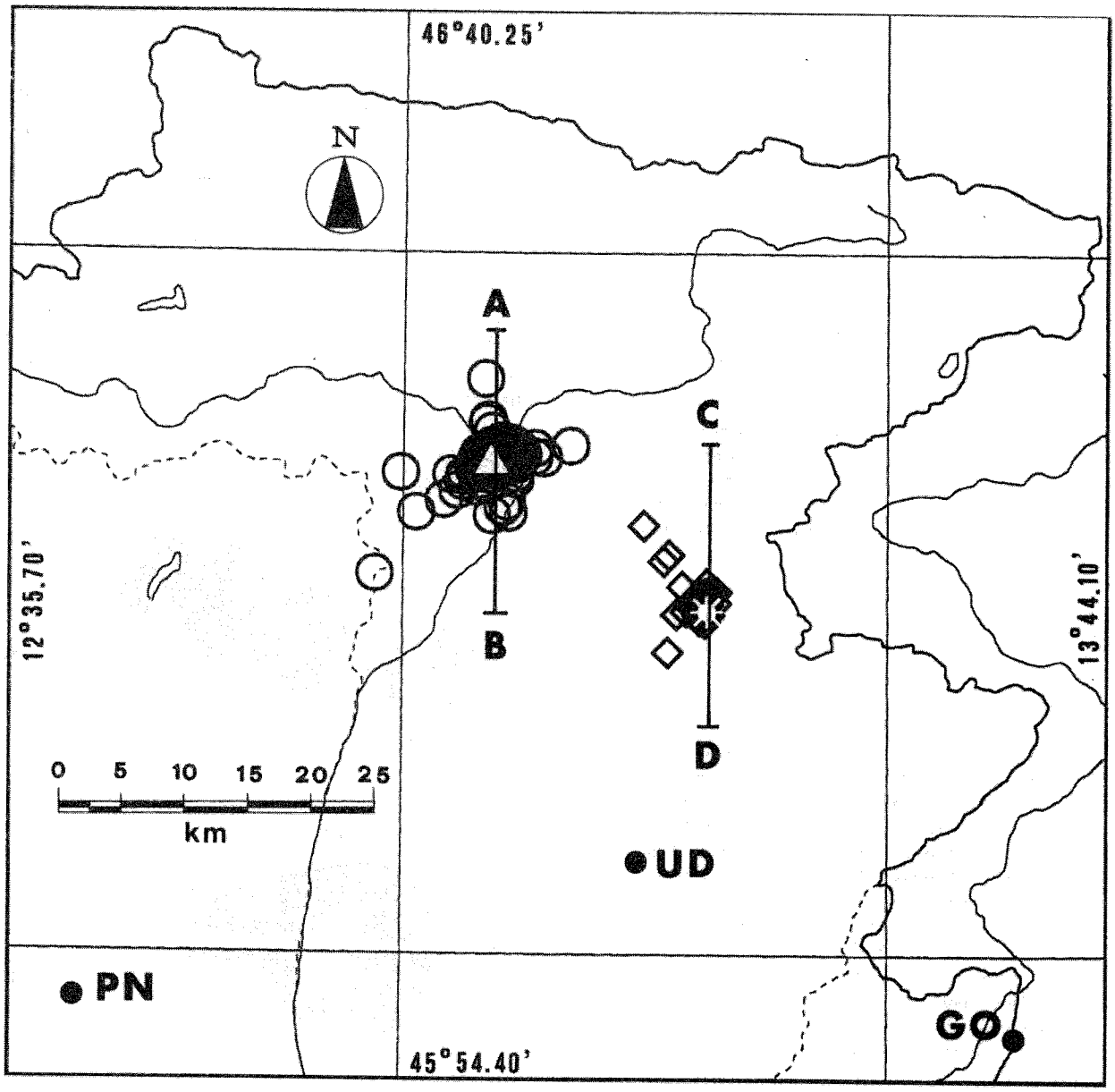

Fig. 2 - Location map of the earthquake aftershock sequences of the present study. Circles: aftershocks following th February 1, 1988 main shock (open triangle). Diamonds: aftershocks following the October 5, 1991 main shock (open asterisk). A-B and C-D: location of vertical cross sections of Fig. 5.

infer the geometrical features and evolution of the hypocentre rupture planes.

The tectonic pattern of the Friuli region (Fig. 3) is characterized by two indented trapezoidal wedges, inherited from the reactivation of early syn-sedimentary fault systems (VENTURINI,1991). These fault systems acted as tectonic constraints during the various tectonic phases. The area affected by the aftershock sequences is

compression related to the neo-Alpine phase (Late Miocene) generated the E-W oriented thrusts and NNE-SSW oriented trascurrent faults intersecting the reverse faults. A NW-SE trending compression followed during Pliocene times, generating NE-SW oriented thrusts. The Plio-Quaternary tectonic activity (CARULLI *et alii*, 1980) is highest in the central sector of the area with uplifting and tilting of the thrust belts and consists in a general

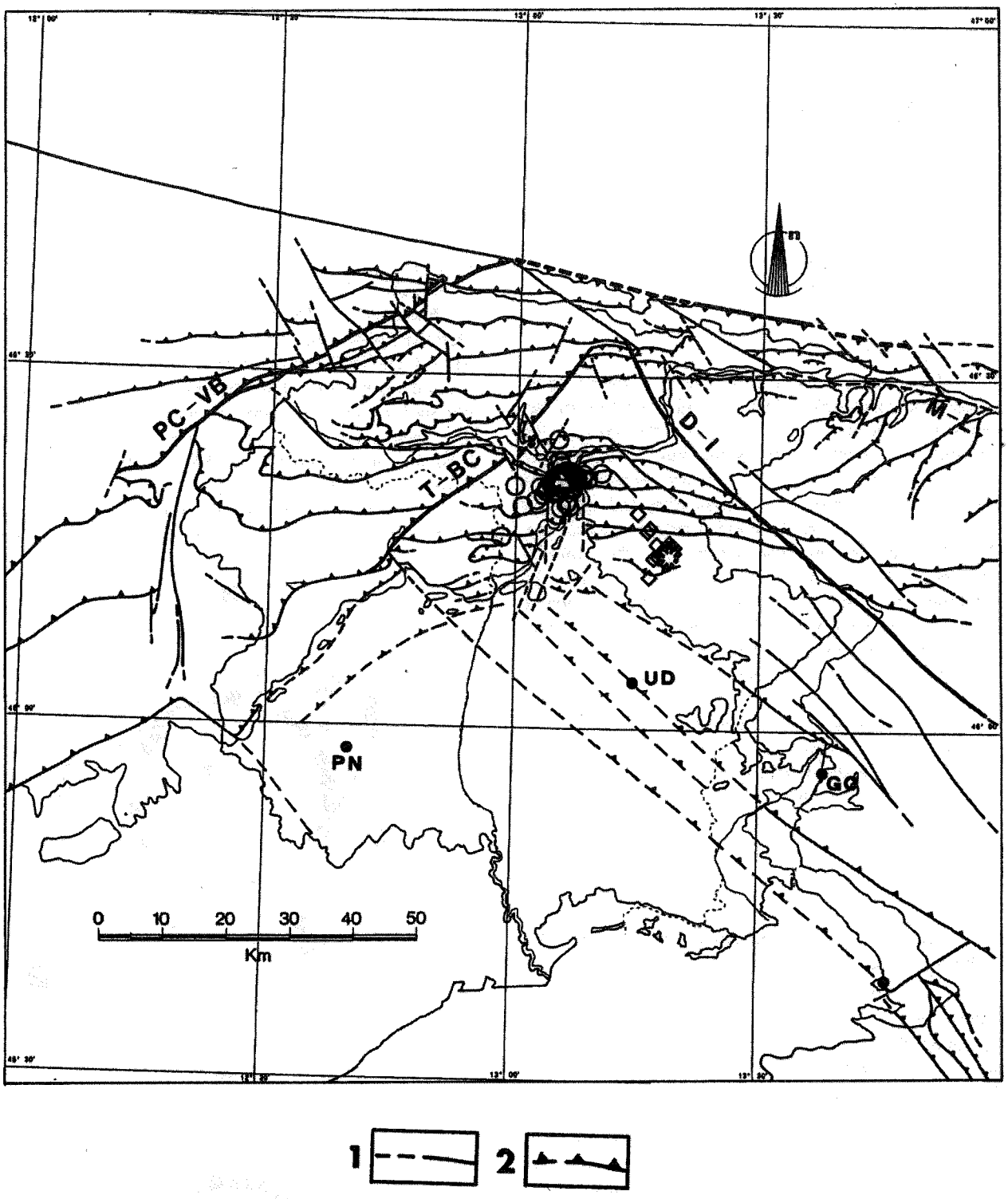

Fig. 3 - Tectonic map of the Friuli area. The aftershock sequences are also plotted (symbols are the same of Fig. 2). 1: sub-vertical fault; 2: thrust. The syn-sedimentary fault systems are enhanced by thickened lines: PC-VB (Pieve di Cadore-Val Bordaglia fault); T-BC (Tramonti-But Chiarsò fault); D-I (Dogna-Idria fault); M-L (Mojstrana-Ljubljana fault). (Modified from VENTURINI, 1991).

NNW-SSE compression. The schematic geological structure of the area consists of a sedimentary cover of mainly Mesozoic units shortened and thickened by thrusting, and detached from a Palaeozoic basement affected by thrusting (SLEJKO *et alii*, 1989).

The seismicity is mostly distributed in the central sector of the area, with maximum concentration between 7 and 11 km depth. The focal mechanisms are mainly of thrust type with a compressional axis oriented from NNW-SSE to N-S (SLEJKO *et alii*,1989) and are related to the Alpine and Dinaric thrusts.

METHOD

The method is based on the calculation of the scatter matrix of the coordinates of a group of events from their centroid (EBBLIN and MICHELINI,1980).

For a set of m hypocentres, the centroid $\overline{x_i}$ is calculated:

$$\bar{X}_i = (1/m)\sum_{k=1}^{m} x_{ki} \quad i = 1,2,3 \qquad (1)$$

with $i = 1,2,3$ spatial coordinates (latitude, longitude and depth) of the k-th event. Then, the scatter matrix of the coordinates of the m events is calculated:

$$l_{ij} = l_{ji} = (1/m)\sum_{k=1}^{m}(x_{ki} - \bar{x}_i)(x_{kj} - \bar{x}_j)$$

$$i, j = 1,2,3 \qquad (2)$$

The matrix represents a spatial ellipsoid fitted through the earthquakes foci. The eigenvectors of the matrix give the spatial orientation of the axes of the ellipsoid; the lengths of the semi-axes are the square roots of the eigenvalues; T_1, T_2, T_3 are respectively the eigenvalues of the maximum, intermediate and minimum axis; and, U_1, U_2 U_3 are the corresponding eigenvectors. The plane of the ellipsoid normal to the smallest eigenvector U_3 is the plane with best fit for the earthquake foci and it represents the quite probable active faulting plane where the seismicity is distributed. The original method has been modified because it generates intermediate fictitious planes placed among the real planes.

The procedure developed by GENTILE (1992) used the following steps:

- The aftershock sequence is divided into minor sub-sequences of n earthquakes.
- For each subsequence of *n* earthquakes, all the combinations of m hypocentres are taken to give:

$$C_{n,m} = \frac{n \cdot (n-1) \cdot (n-2) \cdots (n-m+1)}{1 \cdot 2 \cdots m} \qquad (3)$$

where $C_{n,m}$ are the all possible combination number of n earthquakes, taking m earthquakes at a time.

- For each combination, the centroid $\bar{x}_i$ and the scatter matrix (ellipsoid) of the coordinates are calculated. So $C_{n,m}$ represents the number of ellipsoids, and m is the number of earthquakes for each ellipsoid. The value of m is chosen 6.
- The flat ellipsoids with T_1/T_3 (eigenvalues of maximum and minimum axis) greater than or equal to 100 and $T_1/T_2 \geq 1$ are selected. These values are determined by repeated trials. The threshold limit of the ratio T_1/T_3 is chosen as high as possible to have flattened ellipsoids. In this way the best fitting plane where the hypocentres tend to locate is obtained. The plane normal to the axis U_3 of the ellipsoid represents the plane of the active fault.
- From the obtained ellipsoids, coplanar ellipsoids are grouped and averaged. The search of coplanar ellipsoids enables to recognize planar repetitiveness in the spatial distribution of earthquakes. The azimuth and the dip of U_3 axis are chosen for the conditions of coplanarity. The ellipsoids with the U_3 axis falling inside a range of 30° azimuth and 10° dip are considered to be coplanar. Then, the azimuth and the dip of the U_3 axes of coplanar ellipsoids are averaged.
- The axis U_3 (pole of the active fault plane) corresponding to the most recurrent number (maximum value) of coplanar ellipsoids, for each sub-sequence of n earthquakes, is plotted on a lower hemisphere equal area projection.

DATA ANALYSIS

The analysis is performed on two earthquake sequences, recorded by the local seismological network of the Osservatorio Geofisico Sperimentale, following the February 1, 1988 (local magnitude M_L=4.2) and the October 5,1991 (M_L=3.8) main shocks (Fig. 2 and Fig. 3). All the earthquakes of the analyzed sequences are located using the three-dimensional velocity model obtained for the Friuli area by BRESSAN *et alii*, (1992). The focal mechanisms of the main shocks have been computed with a program of WHITCOMB *et alii*, (1973), based on first P-wave polarities.

The focal mechanism solution of the February 1, 1988 main shock (Fig. 4a) is of thrust type with

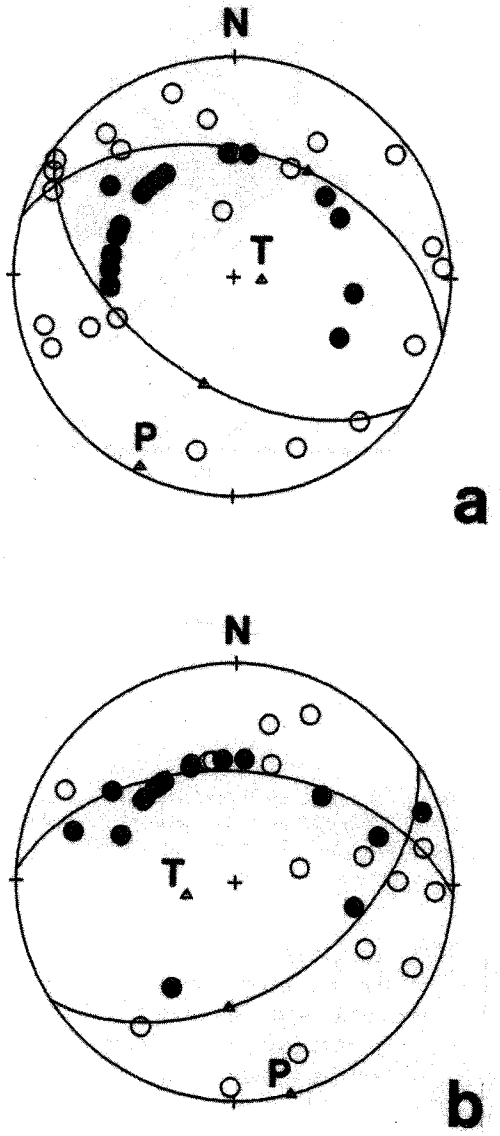

Fig. 4 - Focal mechanism solutions of the February 1, 1988 main shock (a) and the October 5, 1991 main shock (b). Full circles: compression, Open circles: dilatation, P: pressure axis, T: tension axis.

negligible transcurrent component, in accordance with the tectonic framework and could be associated to WNW-ESE active fault dipping 40° to NNE. Focal depth is about 8 km. The analyzed area is 17 km E-W x 18 km N-S; 214 earthquakes for the period up to 54 days after the main shock, and with local magnitude ranging from 1.5 to 3.9 are considered. Fig. 5(1) shows N-S vertical cross-section of the seismicity. The section is normal to the main southverging thrusts of the area. A rough trend (dashed line in Fig. 5(1)) could be recognized and related to the thrusting style of the area. However, the spatial clustering of the earthquakes doesn't allow a unique solution and suggests that aftershocks could be accomodated along multiple branching slip surfaces.

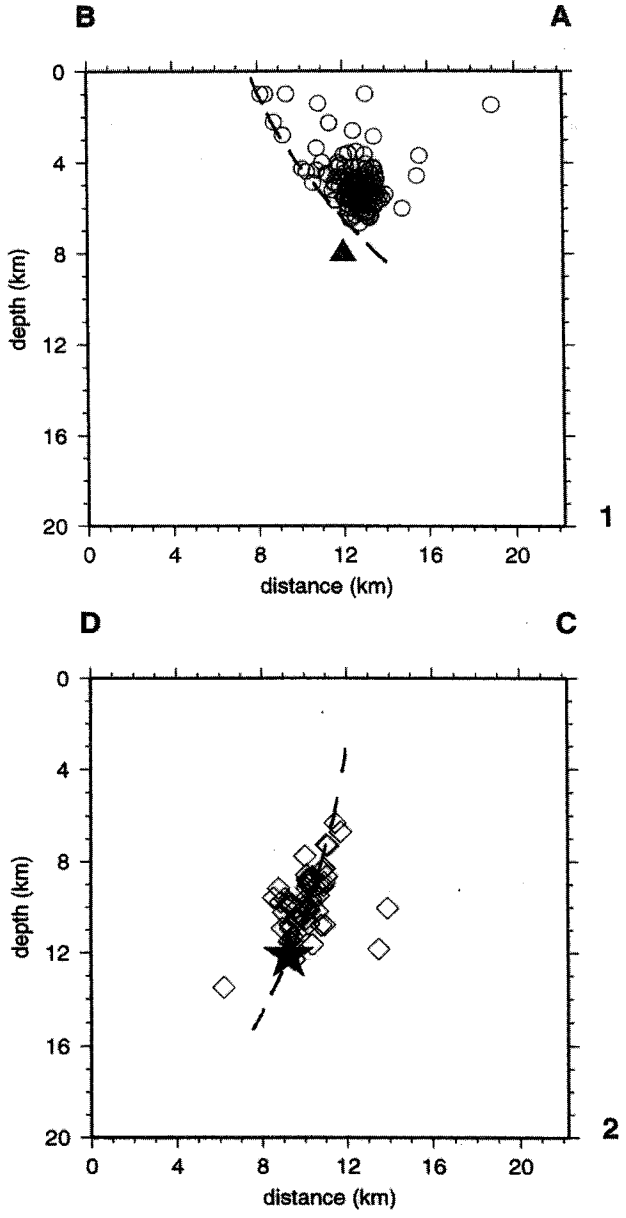

Fig. 5 - N-S vertical cross sections of the aftershock sequences following the February 1,1988 main shock (1) and the October 5, 1991 main shock (2). The main shocks are marked respectively by triangle and star. Dashed lines: rough earthquakes alignment.

It can be supposed that the redistribution of stress following the main shock causes the occurrence of the aftershocks on multiple random planes. The focal depth distribution of the aftershocks (Fig. 6) indicates that the region of seismic strain release is mainly between 4 and 6 km.

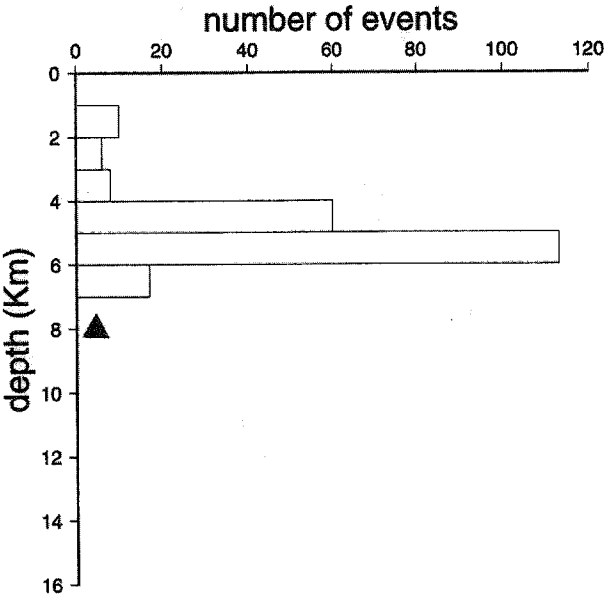

Fig. 6 - Depth distribution of the aftershock sequence of the February 1, 1988 main shock (triangle).

In order to take into account the time evolution, the aftershock sequence is divided into 14 sub-sequences of 15 earthquakes each one, arranged in temporal order. This choice is adopted after repeated trials. It results the better compromise between having a consistent data set to investigate in detail the possible solutions and avoiding heavy computation procedures. The temporal arrangement is performed with the aim to investigate temporal evolution of the sequence. The analysis doesn't change if the sub-sequences are chosen with other criteria, since the used procedure selects the more recurrent coplanar ellipsoids, which represent the best interpolation of the aftershocks preferential fault plane. For each sub-sequence, the eigenvector U_3 (minimum axis) corresponding to the maximum number of coplanar ellipsoids is plotted on a lower hemisphere equal area projection (Fig. 7). A concentration of U_3 axes is recognizable in the SE quadrant, corresponding to a group of planes oriented between N 100°W and N 120°W, with dip ranging between 36° and 80° (planes 4,5,7,8,11,12,13,14). The seismicity is also distributed on other planes with different orientations and dips. The depth of the centroid related to each plane varies between 4 and 5 km. The aftershock subfaults are activated alternately during the sequence. The aftershocks tend to concentrate along nearly WSW-ENE oriented faults dipping to NNW and they are activated by hangingwall deformation above the thrust of the main shock, which strongly focused the energy released.

The October 5, 1991 main shock is characterized by a thrust focal mechanism, with negligible transcurrent component (Fig. 4b) in accordance with the tectonic setting of the area. It could be related to an E-W active fault dipping 45° to the North. The computed focal depth is about 12 km.

The analyzed data consist of 57 aftershocks, with local magnitude ranging from 1.6 to 3.4, an area of 17

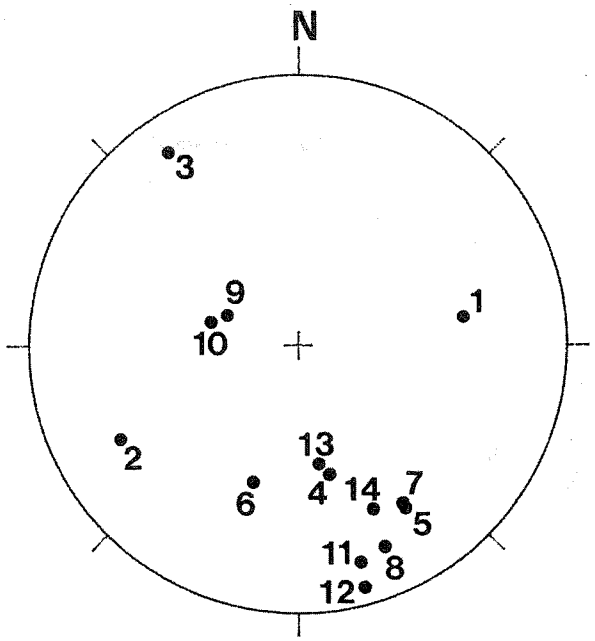

Fig. 7 - Aftershocks of the February 1,1988 earthquake. Lower hemisphere equal area projection of the eigenvectors U_3, corresponding to the maximum number of coplanar ellipsoids for each sequence.

km E-W x 18 km N-S, within a time window of 45 days. The N-S vertical cross-sections (Fig. 5(2)) of the aftershock distribution emphasizes a narrow subvertical zone (dashed line in figure) of stress concentration induced by the main shock, not related to any tectonic structure from the geological evidences of the area. The focal depth distribution (Fig. 8) shows that the region of maximum strain release lies between 8 and 11 km depth.

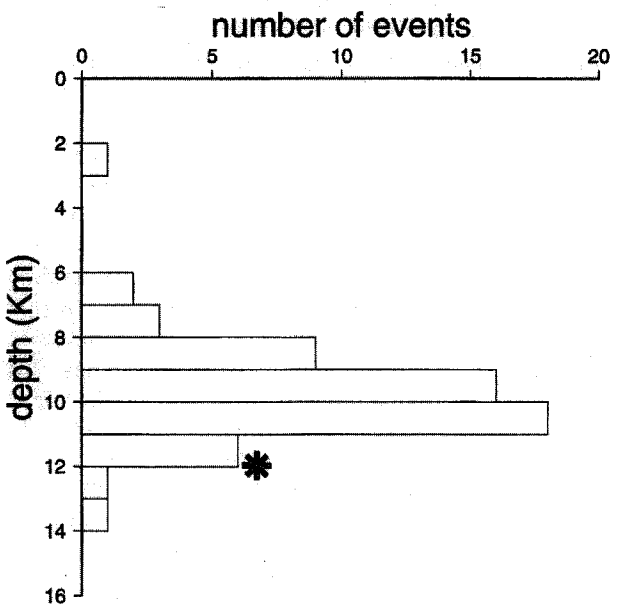

Fig. 8 - Depth distribution of the aftershock sequence of the October 5, 1991 main shock (asterisk).

The aftershock sequence is divided into 6 subsequences of 10 earthquakes each one. Fig. 9 shows the eigenvector U_3 of the maximum number of coplanar ellipsoids on a lower hemisphere equal area projection.

The subsequences 1, 2, 3, 4 and 5 of time-successive hypocentres are distributed on N-S oriented planes, alternately dipping E and W. The planes 1, 2, 3 and 4 are subvertical, and plane 5 is dipping 36° W. The subsequence 6 is located on a subvertical plane, with orientation N 44°W. The depth of the centroid related to each plane varies between 9 and 10 km. The aftershock

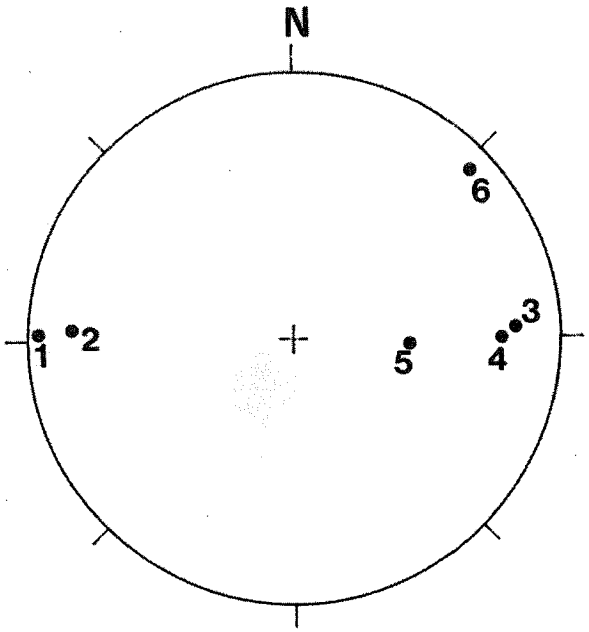

Fig. 9 – Aftershocks of the October 5, 1991 earthquake. Lower hemisphere equal area projection of the eigenvectors U_3, corresponding to the maximum number of coplanar ellipsoids for each sequence

subfaults develop with a conchoidal space pattern and they are activated, like in the previous case, by hangingwall deformation above the thrust of the main shock.

Both aftershock clouds of the analyzed sequences lie over the main shock locations, suggesting that the hypocentral migration is connected with the main fault slip propagation. In these cases, the aftershocks are located on multiple planar structures and they are consistent with an upward stress propagation induced by the main shocks. In accordance with MENDOZA and HARTZELL (1980), the aftershocks occur in the regions near the area of the main shock, and are caused by stress redistribution subsequent to the maximum coseismic displacement. So the space and time clustering of the hypocentres can be explained by the redistribution of local stresses. Every strain (aftershock) drops the energy of the stress field causing a re-orientation of the axes of the deviatoric stress near the border of the fracture. In this way, the aftershocks are related one to each other, with the activated fractures showing different orientations and dips. The random aspect of the aftershock occurrence may also be due to heterogeneities in the physical properties of the rocks (YAMASHITA and KNOPOFF, 1987). The analyzed cases show that the aftershock distribution has to be used with much care to infer the main seismogenic fault.

CONCLUSIONS

Aftershock sequences, which are clustered both in space and time, cannot be satisfactory resolved with a simple single-plane model. The hypocentres are located on multiple planar structures. The geometry of fractures in rock volumes affected by clusters of earthquakes may be resolved by considering the scatter matrix of the coordinates of the hypocentres with respect to their centroid. The aftershock sequence is divided into subsequences, arranged in temporal order. Then the scatter matrix of the earthquake locations, for each subsequence, is computed for a combination of a fixed number of events. The scatter matrix represents a spatial ellipsoid fitted through the aftershock foci. The more recurrent coplanar ellipsoids, selected with an imposed degree of flattening, identify the planar structures where the hypocentres tend to locate.

The results of the analysis performed on two aftershock sequences show that the earthquakes are distributed in proximity to the main shock area and their occurrence is related to the upward stress propagation caused by the main shocks. The spatial orientation of most aftershock subfaults is different from the focal plane of the main shocks, suggesting the following model. The main shocks are caused by the regional NNW-SSE compression and are located on the seismogenic south-verging thrusts. The aftershocks occurred on optimally oriented minor faults for Coulomb failure conditions, that result from the readjustment of local deviatoric stress induced by the main shock, in addition to the regional deviatoric stress, in accordance with King et al. (1994).

Acknowledgments

The seismological network of Friuli is managed by the Dipartimento Centro Ricerche Sismologiche of the Osservatorio Geofisico Sperimentale with financial support from the Regione Autonoma Friuli-Venezia Giulia. The authors wish to thank G. Rossi for details about the principal parameters technique, I. Stanishkova for critically reading the manuscript and S. Urban for elaboration of seismicity figures.

REFERENCES

BRESSAN G., DE FRANCO R. & GENTILE G.F. (1992) - *Seismotectonic study of the Friuli (Italy) area based on tomographic inversion and geophysical data.* Tectonophysics **207**, 383-400.

CARULLI G.B, CAROBENE L., CAVALLIN A., MARTINIS B., & ONOFRI R. (1980) - *Evoluzione strutturale Plio-Quaternaria del Friuli e della Venezia Giulia.* In: Contributi alla realizzazione della Carta Neotettonica d'Italia, parte II. Pubbl. N.356 Prog. Fin. Geodin.-Sottopr. Neotettonica, CNR, 489-545.

DOGLIONI C. & BOSELLINI A. (1987) - *Eoalpine and mesoalpine tectonics in the southern Alps.* Geol. Rundsch., **76**, 3, 735-754.

EBBLIN C. & MICHELINI A. (1986) - *A principal parameters analysis of aftershock sequences applied to the 1977 Friuli, Italy, sequence.* Ann. Geophys., **4**, 473-480.

GENTILE F. (1992) - *Procedura di calcolo per l'analisi della disposizione spaziale dei terremoti nelle zone sismicamente più attive ed, in particolare, nelle sequenze di aftershocks.* Osservatorio Geofisico Sperimentale, rapp. int., n. 9219/CRS-7.

KING G.C.P., STEIN R.S. & LIN J. (1994) - *Static stress changes and the triggering of earthquakes.* Bull. Seism. Soc. Am., **84**, 935-953.

MENDOZA C. & HARTZELL S. (1988) - *Aftershocks patterns and main shock faulting.* Bull. Seism. Soc. Am., **78**, 4, 1438-1449.

SCHOLZ C.H. (1988) - *The mechanics of earthquake and faulting.* Cambridge University Press, 435 pp.

SLEJKO D., CARULLI G.B., CARRARO F., CASTALDINI D., CAVALLIN A., DOGLIONI C., ILICETO V., NICOLICH R., REBEZ A., SEMENZA E., ZANFERRARI A. & ZANOLLA C. (1989) - *Seismotectonics of the Eastern Southern-Alps: a review.* Boll. Geof. Teor. Appl., **XXXI**, 122, 109-136.

VENTURINI C. (1991) - *Cinematica neogenico-quaternaria del sudalpino orientale (settore friulano).* In: Neogene Thrust tectonics. Esempi da Alpi meridionali, Appennino e Sicilia (edited by Boccaletti M., Deiana G. and Papani G.). Studi Geol. Camerti Camerino Vol. spec. 1990, 109-116.

WHITCOMB, J.H., ALLEN, C.R., GARMANY, J.D., & HILEMAN, J.A. (1973) - *San Fernando earthquake series, 1971, focal mechanisms and tectonics.* Rev. Geophys., **11**, 693-730.

YAMASHITA T. & KNOPOFF L. (1987) - *Models of aftershocks occurence.* Geophys. J.R.A.S.,**91**,13-26.